Early magnitude and potential damage zone estimates for the great Mw 9 Tohoku-Oki earthquake

Simona Colombelli,[1] Aldo Zollo,[1] Gaetano Festa,[1] and Hiroo Kanamori[2]

Received 19 September 2012; revised 24 October 2012; accepted 24 October 2012; published 30 November 2012.

[1] The Mw 9.0, 2011 Tohoku-Oki earthquake has re-opened the discussion among the scientific community about the effectiveness of earthquake early warning for large events. A well-known problem with real-time procedures is the parameter saturation, which may lead to magnitude underestimation for large earthquakes. Here we measure the initial peak ground displacement and the predominant period by progressively expanding the time window and distance range, to provide consistent magnitude estimates (M = 8.4) and a rapid prediction of the potential damage area. This information would have been available 35 s after the first P-wave detection and could have been refined in the successive 20 s using data from more distant stations. We show the suitability of the existing regression relationships between early warning parameters and magnitude, provided that an appropriate P-wave time window is used for parameter estimation. We interpret the magnitude under-estimation as a combined effect of high-pass filtering and frequency dependence of the main radiating source during the rupture process. **Citation:** Colombelli, S., A. Zollo, G. Festa, and H. Kanamori (2012), Early magnitude and potential damage zone estimates for the great Mw 9 Tohoku-Oki earthquake, *Geophys. Res. Lett.*, *39*, L22306, doi:10.1029/2012GL053923.

1. Introduction

[2] The Mw 9.0 Tohoku-Oki event represents a unique opportunity to check the extension of present Earthquake Early Warning (EEW) methodologies up to giant earthquakes, to bring out their limits and to propose new strategies to overcome such limitations. The Tohoku-Oki earthquake occurred on March 11th, 2011 at 05:46:24 UTC offshore the North-East coast of Honshu, Japan, at the boundary between the Pacific and the North-American plates (JMA location, http://www.jma.go.jp/jma/menu/jishin-portal.html). The very dense strong motion networks (K-NET, http://www.k-net.bosai.go.jp/ and KiK-net, http://www.kik.bosai.go.jp/) deployed across Japan provided seismic observations over a wide range of distances and azimuths from the source, with a high signal-to-noise ratio in the P-wave Time Window (PTW) up to several hundred kilometers from the source. We have no experience of any other giant earthquake with such a high quality and number of records.

[3] In this work we use two EW parameters, the initial peak ground displacement (P_d) and the predominant period (τ_c) to get rapid estimations of the magnitude and to predict the potential damage of the earthquake. From the analysis of earthquakes in different regions of the world, several authors have found empirical relations between both these parameters and the earthquake size [*Kanamori*, 2005; *Zollo et al.*, 2006; *Böse et al.*, 2007; *Wu and Kanamori*, 2008; *Shieh et al.*, 2008] or between P_d and peak ground velocity and acceleration [*Wu and Kanamori*, 2005; *Zollo et al.*, 2010]. However, these empirical relations were derived and validated using databases limited in magnitude up to 7–7.5 [*Allen and Kanamori*, 2003; *Olson and Allen*, 2005; *Wu and Kanamori*, 2005; *Zollo et al.*, 2010] and may not be suitable for giant events. Furthermore these relationships are based on the analysis of the early P-wave signal of ground motion records in a 3- to 4-second time window. The saturation effect of EW parameters with magnitude within this time window is well known and has been extensively discussed in the literature [*Kanamori*, 2005; *Rydelek and Horiuchi*, 2006; *Rydelek et al.*, 2007; *Zollo et al.*, 2007]. Since the saturation is likely due to the use of only a few seconds of the P-wave which cannot capture the entire rupture process of a large earthquake [*Festa et al.*, 2008], we expect that longer PTWs are required to analyze large events. Another limitation is that the regression relationships among EW parameters and source parameters have been generally applied up to 50–60 km of hypocentral distance, approximately covering the area in which the damaging effects of a moderate-to-large earthquake are expected. Such a distance range is too restricted for a magnitude Mw 9.0 earthquake, like the 2011 Tohoku-Oki earthquake, which was felt as "very strong" up to about 300 km [*Hoshiba et al.*, 2011]. Finally, the acceleration data processing requires a high-pass filter to remove baseline effects caused by the double integration (see next section). While removing the artificial distortions, filters also reduce the low frequency content of the recorded waveforms and may change the scaling between early measurements and the final magnitude.

[4] Here we want to investigate the reliability of existing EW methodologies and empirical regression relations for the Tohoku-Oki earthquake. For the same earthquake, *Hoshiba and Iwakiri* [2011] analyzed the initial peak ground motion and the τ_c parameter in the first 30 s after the first arrival at four accelerometric stations along the coast. Here we generalize this approach by expanding the analysis to larger PTW (up to 60 s) and epicentral distances (up to 530 km), showing that the early measurements of P-peak displacement and τ_c at the whole Japanese accelerometric network provided relevant insights on the ongoing earthquake

[1]Dipartimento di Scienze Fisiche, Università di Napoli Federico II, Naples, Italy.
[2]Seismological Laboratory, California Institute of Technology, Pasadena, California, USA.

Corresponding author: A. Zollo, Dipartimento di Scienze Fisiche, Università di Napoli Federico II, I-80125 Naples, Italy. (aldo.zollo@unina.it)

©2012. American Geophysical Union. All Rights Reserved.
0094-8276/12/2012GL053923

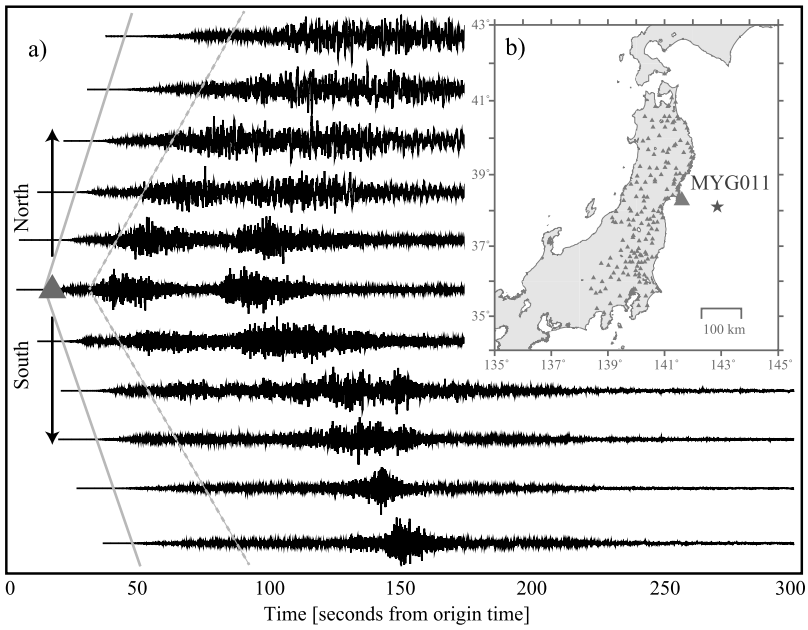

Figure 1. Data. (a) Example of acceleration waveforms arranged as a function of distance with respect to the closest station, MYG011 (represented through a larger size triangle); the approximate theoretical P (solid line) and S-waves (dashed line) arrival times are also shown. (b) Distribution of Kik-Net and K-NET stations (gray triangles) used in this work. The JMA earthquake location is represented through a black star.

rupture process and reliable estimations of the potential damage area.

2. Preliminary Analysis

[5] We analyzed 546, 3-component strong motion accelerometer records for the Tohoku-Oki earthquake, in the distance range between 120 and 530 km from the epicenter; waveforms were extracted from the KiK-net and K-NET databases. Figure 1 shows a sample of waveforms (Figure 1a) and the distribution of selected stations (Figure 1b). We measured the initial peak displacement, P_d, and the predominant period, τ_c, after single and double integration to get velocity and displacement, respectively. For real-time applications a causal 2-pole Butterworth, high-pass filter with a cut-off frequency of 0.075 Hz is usually applied to remove undesired long-period trends and baselines introduced by double integration [*Boore et al.*, 2002]. *Zollo et al.* [2010] have shown that this cut-off frequency preserves a scaling of the EW parameters with magnitude in a broad range ($4 < M < 7$). This frequency is lower or comparable to the corner frequency of any seismic event in the analyzed magnitude range, allowing to capture the low-frequency coherent radiation from the source. However, for giant earthquakes the expected corner frequency is significantly smaller than such a cut-off filtering frequency; a preliminary study is then required to evaluate the effect of high-pass filtering on the Tohoku-Oki records and of the expansion of the PTW.

[6] We tested 80 combinations of cut-off frequencies and PTWs, from 0.001 Hz to 0.07 Hz and from 3 to 30 s, respectively. To avoid the S-wave contamination while increasing the PTW we computed the theoretical S-wave arrival times and excluded from our analysis all the stations for which the estimated S-wave arrival occurred within the considered PTW. While expanding the PTW the closest stations are hence excluded one by one during the analysis. Furthermore, in order to compare the average P_d values for different stations, these have to be corrected for the geometrical attenuation effect. Using an independent dataset of Japanese, Taiwan and Italian earthquakes (3552 records corresponding to 296 events in the range of magnitude $4 < M < 8.4$ and distance $R < 200$) and through a linear regression analysis, we derived the coefficients of the following attenuation relationship:

$$\log P_d = -3.59(\pm 0.09) + 0.73(\pm 0.09) \cdot M - 1.14(\pm 0.05) \cdot \log R \quad (1)$$

where P_d is measured in centimeters, M is the magnitude and R is the hypocentral distance in kilometers. These coefficients were used to correct the displacement for the distance effect and to normalize all the measured values to a reference distance of 100 km. We then computed the average P_d and τ_c values as a function of the cut-off frequency for different PTWs. Results are shown in Figures S1a and S1b in the auxiliary material.[1] We found that both parameters vary with the cut-off frequency with a similar trend. Both P_d and τ_c assume the largest values for small cut-off frequencies and large PTWs and their logarithm decreases almost linearly with the cut-off frequency for each considered PTW. This behavior suggests that, independently of the cut-off filtering frequency, $\log(\tau_c)$ [or $\log(P_d)$] may be used for estimating the magnitude, provided that proper scaling coefficients are determined from the data. For the sake of uniformity with the previous works and since the empirical relationships used in this work were obtained with a 0.075 Hz cut-off

[1]Auxiliary materials are available in the HTML. doi:10.1029/2012GL053923.

frequency, we decided to maintain this value for the filtering operation.

3. Expanding the P-Wave Time Window: Evidence for Parameter Saturation

[7] We measured the EW parameters using different PTWs, from 3 to 60 s for all the available records, using the procedure discussed above. Our aim is to understand whether the problem of magnitude underestimation due to parameter saturation may be overcome using appropriate PTWs and if the empirical regression relations relating EW parameters and magnitude are still valid for this event. The saturation effect on P_d and τ_c measurements in short PTWs is well evident from data. Figures 2a and 2b show the mean value and standard deviation of P_d and τ_c within progressively increasing time windows measured after the first P-arrival. We again exclude data possibly contaminated by the S-wave arrival and correct P_d estimates for the distance, according to equation (1). As for the peak displacement (Figure 2a), it regularly increases with PTW, reaching a plateau at about 25–30 s, this corresponding to hypocentral distances greater than 240 km. From equation (1), the mean value of magnitude for PTW ≥ 30 s is M = 8.4 ± 0.2. The average period, τ_c, (Figure 2b) shows a similar behavior although the errors on measurements at each PTW are much larger than those found for P_d. The average τ_c increases with PTW and becomes constant after 25–30 s at a mean value which again corresponds to M = 8.4 ± 0.2 according to the τ_c vs. Mw relationship [*Zollo et al.*, 2010]. In both plots, error bars represent the standard deviation associated with each value; they depend on the scatter of the measurements but also on the number of observations, which decreases with increasing PTW. The final values of magnitude estimated from P_d and τ_c are consistent within error bars, suggesting that more robust estimations can be obtained by the combined use of amplitude and period parameters.

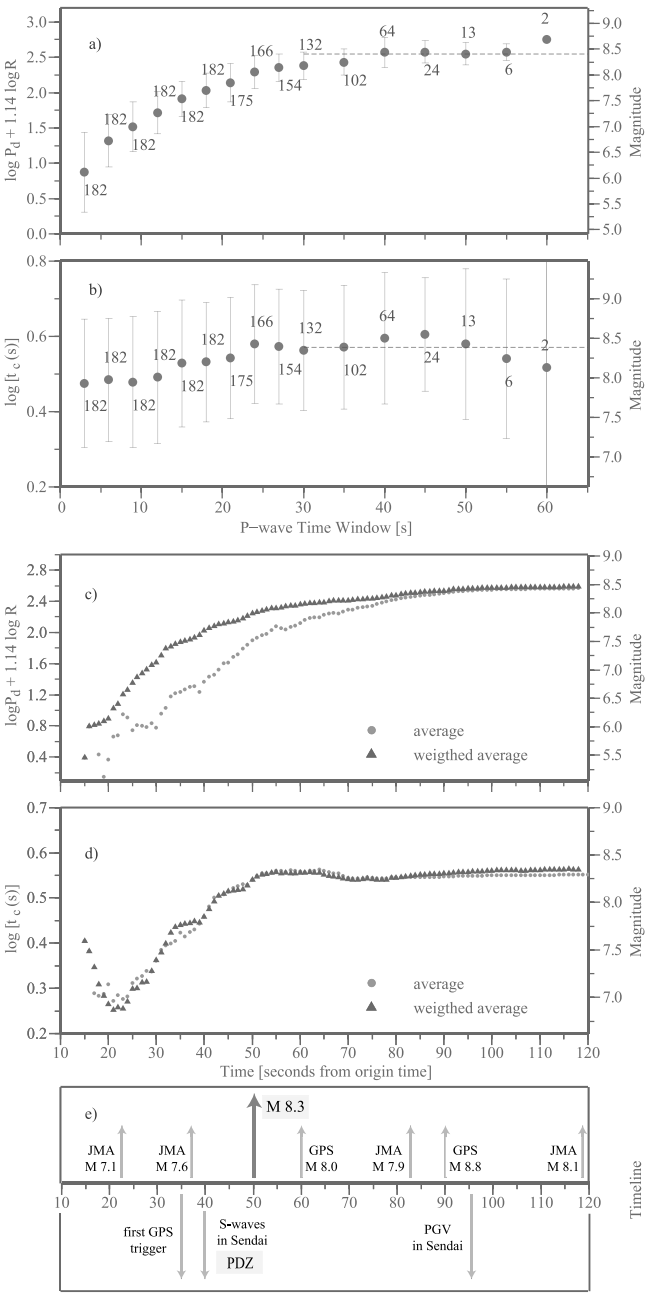

Figure 2. Average values of (a) P_d and (b) τ_c as a function of the P-wave Time Window used. Error bars are computed as the standard deviation associated to each value; the gray number close to each point represents the number of stations used for each considered time window. Both parameter exhibit saturation when a 25–30 s PTW is used: the final saturation level (PTW ≥ 30 s) is shown by the gray dashed lines. Real-time evolution of (c) P_d and (d) τ_c as a function of time from the origin time. In each plot, gray circles represent the standard average values while triangles are the result of the weighted average computation. Each weight is proportional to the square of the PTW, so that the longer the available record, the more relevant the contribution to the computation. For each plot, the corresponding magnitude scale is also represented; this has been derived based on the coefficients of equation (1) and on the τ_c vs. M relationship determined by *Zollo et al.* [2010]. (e) Comparison of our evolutionary magnitude estimation with the warning issued by the JMA agency and with the magnitude estimates from 1 Hz GPS data [*Wright et al.*, 2012]. The timeline also shows when our magnitude estimates would have been available relative to the arrival of S-waves and of the strongest shaking (labeled as "PGV in Sendai") along the coast.

4. Real-Time Analysis

[8] The available PTW at each time step and recording site depends on the P-wave propagation and on the apparent velocity through the seismic network. To use our approach in real-time EW applications, we reordered P_d and τ_c measurements as a function of time from the event Origin Time (OT), as it is usually done in EW systems. We maintained the idea of the expanding PTW and, at the same time, we considered the delayed P-wave arrival time as a function of distance. In the previous analysis we used the same PTW for all the stations; here, instead, we use the maximum PTW available for each triggered station, i.e., the time interval between the observed P-wave arrival time and the theoretical S-wave arrival time. In this way all the stations contribute to the measurement, with shorter PTWs for nearby stations and longer PTWs for more distant stations. Results obtained

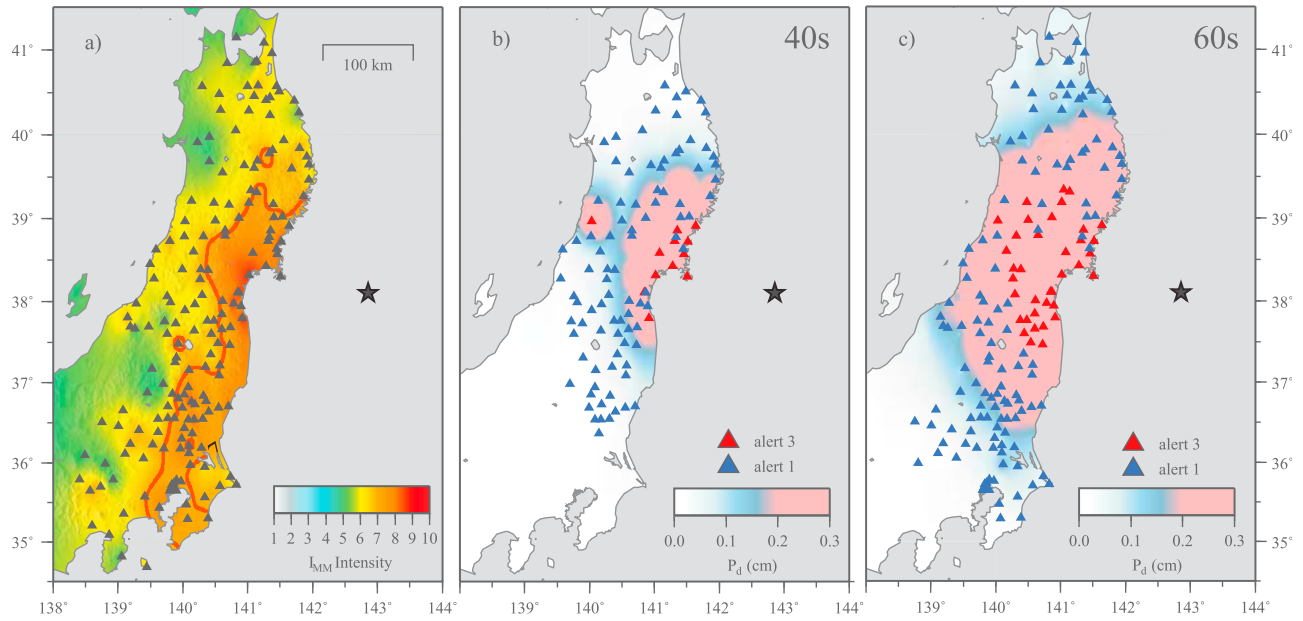

Figure 3. Comparison between (a) the real Instrumental Intensity (I_{MM}) distribution and the predicted P_d distribution that would have been available (b) 40 and (c) 60 s after the OT. The Instrumental Intensity distribution (Figure 3a) has been obtained from the observed Peak Ground Velocity at all the available stations, using the conversion table of *Wald et al.* [1999]. Figures 3b and 3c show the distribution P_d values, obtained after interpolating measured and predicted initial displacement values. The color transition from light blue to red represents the P_d = 0.2 cm isoline, which corresponds to a I_{MM} = 7, based on the scaling relationship of equation (1) in *Zollo et al.* [2010]. The available stations at each time are plotted with red and blue triangles, based on the local alert level.

from this analysis are plotted in Figures 2c and 2d (gray circles) and show that the general trend of average P_d and τ_c is similar to that of Figures 2a and 2b, both parameters providing evidence for saturation around 50 s from OT. A possible risk when averaging values resulting from windows with different lengths is that stations with short PTWs can provide a magnitude underestimation affecting the mean value. In order to reduce this effect, at each considered time step we computed weighted averages of P_d and τ_c, with a weight proportional to the square of the window length (dark triangles in Figures 2c and 2d). With this approach we found a significant increase of the initial average values of P_d, while the effect is less evident on τ_c, being probably hidden by the intrinsic larger variability of this parameter. In both cases, however, the final average magnitude values are consistent with the results of the previous analysis (Figures 2a and 2b).

[9] Beyond the real-time magnitude estimation another relevant goal of an EEW system is the rapid identification of the Potentially Damaged Zone (PDZ) and prompt broadcasting of a warning in the highest vulnerable areas before the arrival of the strongest shaking, so that security actions can be rapidly activated (i.e., automatic shut down of pipeline and gas line, …). Following the same methodology as described in *Colombelli et al.* [2012], and using the empirical scaling relationship of *Zollo et al.* [2010] (equation (4)), we estimated the P_d distribution for the whole territory of Japan, by interpolating the observed P_d values at close-in stations and the predicted P_d values at more distant sites. In Figure 3 we compare the Instrumental Intensity (I_{MM}) distribution (Figure 3a) with the predicted P_d distribution that would have been available 40 (Figure 3b) and 60 s (Figure 3c) after the OT. The Instrumental Intensity distribution (Figure 3a) has been obtained from the observed Peak Ground Velocity at all the available stations, using the conversion table of *Wald et al.* [1999]. In Figure 3b and 3c, the stations for which measured values of P_d and τ_c are available are plotted with red and blue triangles; the color represents the local alert level that would have been assigned to each recording site, following the scheme proposed by *Zollo et al.* [2010]. The alert levels can be interpreted in terms of potential damaging effects nearby the recording station and far away from it. For instance, an alert level 3 corresponds to an earthquake likely to have a large size and to be located close to the recording site, thus a high level of damage is expected both nearby and far away from the station. The PDZ of Figure 3b is fairly consistent with the area where the highest intensity values are observed (i.e., I_{MM} > 7, red contour line). Although the first reliable mapping of the P_d distribution is available 40 s after OT, the local alert levels at the coastal stations are available well before (two alert level 3 at the closest stations are available 25 s after the OT); this information can be used to issue a warning, despite the magnitude estimation has not yet reached its final value. A stable P_d distribution is finally available later in time, around 60 s after OT (Figure 3c). However, in the southern part of Japan (Tokyo region) the intensity values are not well reproduced, probably due to a significant contribution of the late peak arrivals radiated by the late activated asperities located southward the epicenter, and which mostly affected this area.

5. Discussion and Conclusive Remarks

[10] Although the complexity of the rupture process for large earthquakes has not yet been fully understood, the

application of EW methodologies to the Tohoku-Oki strong motion records can represent a useful tool to reveal new insights into the very delicate issue of early magnitude estimation for large earthquakes and the prediction of the potential damage area while the rupture process is still ongoing. The analysis performed in this work provided relevant implications for both the physical properties of the seismic source and the more practical aspects related to the implementation of real-time EW methodologies for large events.

[11] As for the first aspect, the evolutionary estimation of P_d and τ_c as a function of the PTW showed that the existing methodologies and regression relationships commonly used for EW applications can be extended even to this large earthquake, provided that appropriate time and distance windows are selected for the measurements. We found that P_d and τ_c are indeed largely underestimated when a small PTW (a few seconds) is used while stable and consistent values are obtained for PTW exceeding 25–30 s. It has to be noted that, although the average values are well consistent, the strong variability of τ_c makes the uncertainties on this parameter at each PTW much larger than those on P_d. The scaling between these two EW parameters and the magnitude remains the same as for $M < 7$ earthquakes, allowing for a correct real-time evaluation of the event size.

[12] This study extends the analysis of *Hoshiba and Iwakiri* [2011], by overcoming the limitation owing to the use of the closest four accelerometric stations along the coast (at a maximum epicentral distance of 164 km). For such stations the S-waves are expected to arrive within the selected 30 s time window and their inclusion within the PTW may introduce a significant bias in magnitude estimations because of a different scaling between magnitude and early warning parameters for P- and S-waves [*Zollo et al.*, 2006]. Furthermore, the limited distance range analyzed by *Hoshiba and Iwakiri* [2011] is expected to provide a partial image of the ongoing source process, whose full investigation requires broader time and distance/azimuth ranges. We came to the conclusion that both P_d and τ_c estimate an earthquake magnitude $M > 8$ when using large PTWs (>25 s), although uncertainties in magnitude estimation from P_d ($\sim$0.3) are significantly smaller than the uncertainties from τ_c ($\sim$1.0).

[13] As for the magnitude estimation of Tohoku-Oki earthquake P_d and τ_c exhibit a saturation effect and provide a magnitude estimation of $M = 8.4$. Since the final earthquake magnitude is Mw 9.0, does this smaller value reflect the magnitude of the early portion of the event or is it an artifact due to uncertainties in the empirical regression laws and/or to measurement procedures? Kinematic inversions for this earthquake have shown a complex frequency dependent rupture history, with asperities radiating energy with different frequency content at different locations [*Meng et al.*, 2011]. The moment rate function [*Lee et al.*, 2011] can be used as a proxy for the far-field P-wave displacement if the finite fault effects such as directivity and changes in the focal mechanism are neglected. The three principal peaks of the moment-rate function have been interpreted as different slip episodes which occurred on the plate boundary interface. The first one occurred near the hypocentral area, the second in the shallower part of the plate boundary interface close to the trench and the last one in the southern part of the fault [*Ide et al.*, 2011; *Koketsu et al.*, 2011; *Maercklin et al.*, 2012]. The duration of the three episodes is different, with the longest one lasting 50–80 s. The saturation observed in the P_d vs. PTW plot (Figures 2a and 2b) beyond 30 s probably corresponds to the end of the first rupture episode. Since the second rupture episode appears to be deficient in high-frequency (>0.05 Hz) energy radiation [e.g., *Ishii*, 2011], we therefore suggest that the 0.075 Hz high-pass filter used for the evolutionary estimation of P_d and τ_c captured the energy from the first event while filtering out the prominent energy emitted from the second one, thus leading to a smaller magnitude, 8.4, when compared to the final earthquake size. However, consistency of P_d and τ_c (Figures 2c and 2d) with the shape of moment rate time function of *Lee et al.* [2011] in the initial 30 s of rupture suggests that early warning parameters provide an evolutionary image of the ongoing fracture process.

[14] Despite of the final magnitude underestimation we note that, for the Tohoku-Oki earthquake, the high-pass filtering did not prevent a correct evaluation of the PDZ. The prediction of the PDZ becomes stable about 40 s after the OT. This study suggests that records at distances up to several hundred kilometers from the earthquake epicenter help in constraining the magnitude estimation obtained from near-source data. However, the maximum distance to be considered needs to be properly defined as a function of the signal-to-noise ratio, which decreases with epicentral distance and event size. Automatic selection of the proper PTW can be achieved, for example, by increasing the PTW until both P_d and τ_c parameters stabilize, i.e., until no significant variations are observed. In order to account for the uncertainties on P_d and τ_c, appropriate strategies to combine these two parameters could be adopted, such as Bayesian probabilistic approaches as proposed by *Lancieri and Zollo* [2008]). Furthermore, an initial location of the hypocenter is required, in order to correctly estimate the S-wave arrival time, and to exclude data at stations for which the S-waves are expected to arrive within the selected PTW.

[15] The proposed evolutionary approach based on gradually increasing PTWs provides, for the Tohoku-Oki earthquake, stable magnitude estimations within 45–50 s after the OT. The availability of real-time measurements of P_d and τ_c at the closest stations allows for a rapid prediction of the expected ground motion at stations located far away from the source area and for a rapid estimation of the PDZ. Following the timeline of Figure 2e, this information would have been released approximately at the time of the S-wave arrival along the coast (Sendai area); however, since the Tohoku-Oki earthquake epicenter was about 120 km offshore, it took more than a minute before the strongest shaking arrived in the same area (labeled as "PGV in Sendai" along the timeline). Thus, longer PTWs would have not diminished the usefulness for early warning in that case.

[16] Finally, in Figure 2e we compare our evolutionary magnitude estimation to the warning issued by the JMA agency and to the estimation based on 1 Hz GPS data [from *Wright et al.*, 2012]. We found that our magnitude estimation, although smaller than the final one, is significantly larger than early estimations provided by both JMA standard procedures and GPS data within the same time window.

[17] **Acknowledgments.** This work was financially supported by Dipartimento della Protezione Civile (DPC) through AMRA scarl within the research contracts REAC and RELUIS 2010–2013, and by EU-FP7 in the framework of project REAKT. We are grateful to Anthony Lomax

and to an anonymous reviewer for their valuable and constructive comments.

[18] The Editor thanks two anonymous reviewers for their assistance in evaluating this paper.

References

Allen, R. M., and H. Kanamori (2003), The potential for earthquake early warning in Southern California, *Science*, *300*, 786–789, doi:10.1126/science.1080912.

Boore, D. M., C. D. Stephens, and W. B. Joyner (2002), Comments on baseline correction of digital strong-motion data: Examples from the 1999 Hector Mine, California, earthquake, *Bull. Seismol. Soc. Am.*, *92*, 1543–1560, doi:10.1785/0120000926.

Böse, M., C. Ionescu, and F. Wenzel (2007), Earthquake early warning for Bucharest, Romania: Novel and revised scaling relations, *Geophys. Res. Lett.*, *34*, L07302, doi:10.1029/2007GL029396.

Colombelli, S., O. Amoroso, A. Zollo, and H. Kanamori (2012), Test of a threshold-based earthquake early warning using Japanese data, *Bull. Seismol. Soc. Am.*, *102*, 1266–1275, doi:10.1785/0120110149.

Festa, G., A. Zollo, and M. Lancieri (2008), Earthquake magnitude estimation from early radiated energy, *Geophys. Res. Lett.*, *35*, L22307, doi:10.1029/2008GL035576.

Hoshiba, M., and K. Iwakiri (2011), Initial 30 seconds of the 2011 off the Pacific coast of Tohoku earthquake (*M*w 9.0) -amplitude and τc for magnitude estimation for earthquake early warning, *Earth Planets Space*, *63*, 547–551, doi:10.5047/eps.2011.05.031.

Hoshiba, M., K. Iwakiri, N. Hayashimoto, T. Shimoyama, K. Hirano, Y. Yamada, Y. Ishigaki, and H. Kikuta (2011), Outline of the 2011 off the Pacific coast of Tohoku earthquake (Mw 9.0)—Earthquake early warning and observed seismic intensity-, *Earth Planets Space*, *63*, 547–551, doi:10.5047/eps.2011.05.031.

Ide, S., A. Baltay, and G. C. Beroza (2011), Shallow dynamic overshoot and energetic deep rupture in the 2011 M_w 9.0 Tohoku-Oki earthquake, *Science*, *332*, 1426–1429, doi:10.1126/science.1207020.

Ishii, M. (2011), High-frequency rupture properties of the *M*w 9.0 off the Pacific coast of Tohoku earthquake, *Earth Planets Space*, *63*, 609–614, doi:10.5047/eps.2011.07.009.

Kanamori, H. (2005), Real-time seismology and earthquake damage mitigation, *Annu. Rev. Earth Planet. Sci.*, *33*, 195–214, doi:10.1146/annurev.earth.33.092203.122626.

Koketsu, K., et al. (2011), A unified source model for the 2011 Tohoku earthquake, *Earth Planet. Sci. Lett.*, *310*, 480–487, doi:10.1016/j.epsl.2011.09.009.

Lancieri, M., and A. Zollo (2008), A Bayesian approach to the real time estimation of magnitude from the early P- and S-wave displacement peaks, *J. Geophys. Res.*, *113*, B12302, doi:10.1029/2007JB005386.

Lee, S. J., B. S. Huang, M. Ando, H. C. Chiu, and H. J. Wang (2011), Evidence of large scale repeating slip during the 2011 Tohoku-Oki earthquake, *Geophys. Res. Lett.*, *38*, L19306, doi:10.1029/2011GL049580.

Maercklin, N., G. Festa, S. Colombelli, and A. Zollo (2012), Twin ruptures grew to build up the giant 2011 Tohoku, Japan, earthquake, *Sci. Rep.*, *2*, 709, doi:10.1038/srep00709.

Meng, L. S., A. Inbal, and J. P. Ampuero (2011), A window into the complexity of the dynamic rupture of the 2011 Mw 9 Tohoku-Oki earthquake, *Geophys. Res. Lett.*, *38*, L00G07, doi:10.1029/2011GL048118.

Olson, E. L., and R. M. Allen (2005), The deterministic nature of earthquake rupture, *Nature*, *438*, 212–215, doi:10.1038/nature04214.

Rydelek, P., and S. Horiuchi (2006), Is earthquake rupture deterministic?, *Nature*, *442*, E5–E6, doi:10.1038/nature04963.

Rydelek, P., C. Wu, and S. Horiuchi (2007), Comment on "Earthquake magnitude estimation from peak amplitudes of very early seismic signals on strong motion records" by Aldo Zollo, Maria Lancieri, and Stefan Nielsen, *Geophys. Res. Lett.*, *34*, L20302, doi:10.1029/2007GL029387.

Shieh, J. T., Y. M. Wu, and R. M. Allen (2008), A comparison of τ_c and τ_p^{max} for magnitude estimation in earthquake early warning, *Geophys. Res. Lett.*, *35*, L20301, doi:10.1029/2008GL035611.

Wald, D. J., V. Quitoriano, T. H. Heaton, and H. Kanamori (1999), Relationships between peak ground acceleration, peak ground velocity and modified Mercalli intensity in California, *Earthquake Spectra*, *15*, 557–564, doi:10.1193/1.1586058.

Wright, T. J., N. Houlié, M. Hildyard, and T. Iwabuchi (2012), Real-time, reliable magnitudes for large earthquakes from 1 Hz GPS precise point positioning: The 2011 Tohoku-Oki (Japan) earthquake, *Geophys. Res. Lett.*, *39*, L12302, doi:10.1029/2012GL051894.

Wu, Y. M., and H. Kanamori (2005), Experiment of an on-site method for the Taiwan Early Warning System, *Bull. Seismol. Soc. Am.*, *95*, 347–353, doi:10.1785/0120040097.

Wu, Y. M., and H. Kanamori (2008), Development of an earthquake early warning system using real-time strong motion signals, *Sensors*, *8*, 1–9, doi:10.3390/s8010001.

Zollo, A., M. Lancieri, and S. Nielsen (2006), Earthquake magnitude estimation from peak amplitudes of very early seismic signals on strong motion, *Geophys. Res. Lett.*, *33*, L23312, doi:10.1029/2006GL027795.

Zollo, A., M. Lancieri, and S. Nielsen (2007), Reply to comment by P. Rydelek et al. on "Earthquake magnitude estimation from peak amplitudes of very early seismic signals on strong motion records," *Geophys. Res. Lett.*, *34*, L20303, doi:10.1029/2007GL030560.

Zollo, A., O. Amoroso, M. Lancieri, Y. M. Wu, and H. Kanamori (2010), A threshold-based earthquake early warning using dense accelerometer networks, *Geophys. J. Int.*, *183*, 963–974, doi:10.1111/j.1365-246X.2010.04765.x.